ASIAN JOURNAL OF PHARMACEUTICAL SCIENCES 12 (2017) 179–186

Available online at www.sciencedirect.com

ScienceDirect

journal homepage: www.elsevier.com/locate/ajps

Original Research Paper

Preparation of CaP/pDNA nanoparticles by reverse micro-emulsion method: Optimization of formulation variables using experimental design

Wenpan Li, Shasha Jing, Xiu Xin, Xirui Zhang, Kang Chen, Dawei Chen, Haiyang Hu *

Department of Pharmaceutics, School of Pharmacy, Shenyang Pharmaceutical University, No. 103, Wenhua Road, Shenyang 110016, China

ARTICLE INFO

Article history:
Received 21 June 2016
Received in revised form 26 August 2016
Accepted 27 September 2016
Available online 4 November 2016

Keywords:
CaP nanoparticles
pDNA
Reverse microemulsion method
Box–Behnken design
Transfection and expression

ABSTRACT

In this study, the CaP/pDNA nanoparticles were prepared using Triton X-100/Butanol/Cyclohexane/Water reverse microemulsion system. Optimization of preparation conditions was based on evaluation of particle size by Box–Behnken design method. The particle sizes of the optimized CaP/pDNA nanoparticles were found to be 60.23 ± 4.72 nm, polydispersity index was 0.252 and pDNA encapsulate efficiency was more than 90%. The optimized CaP/pDNA nanoparticles have pH sensitivity and biocompatibility. Further, optimized CaP/pDNA nanoparticles showed higher transfection efficiency.

1. Introduction

Calcium phosphate (CaP) has been widely used as a gene carrier to mediate pDNA into mammalian cells [1,2] because of its good biocompatibility, biodegradability, as well as easy handling and preparation [3]. However, there exist many factors that affect the transfection of CaP, especially the size and size distribution of CaP play an important role in the transfection progress [4]. According to previous reports, small particle size was beneficial to cell transfection and expression; in addition, nano-sized non-agglomerated precipitate is a key parameter for effective calcium phosphate nanoparticle transfection [5] .

In order to get uniform nanoparticles, many size-controlled methods have been reported, including precipitation method, hydrothermal method, sol process, autocombustion method and reverse microemulsion method [6,7]. The size and size distribution of CaP are difficult to control by means of the chemical

* *Corresponding author.* Shenyang Pharmaceutical University, No. 103, Wenhua Road, Shenyang 110016, China. Fax: +86 24 23986306.
E-mail address: haiyang_hu@hotmail.com (H. Hu).
Peer review under responsibility of Shenyang Pharmaceutical University.
http://dx.doi.org/10.1016/j.ajps.2016.09.006

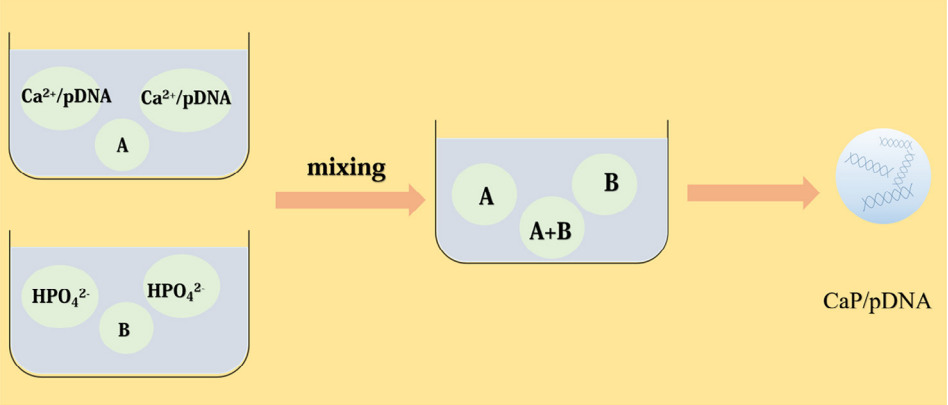

Fig. 1 – Schematic diagram of nanoparticle preparation by microemulsion.

precipitation and hydrothermal methods due to the fast nucleation, aggregation and subsequent anisotropic growth of crystal faces [7]. Rapid growth of the particles resulting in sharp increase in diameter is thus a big hurdle which must be eliminated for efficient gene delivery and expression into the cells [8].

The reverse microemulsion method is an effective approach to regulate the size and size distribution of CaP crystals, which can restrict strictly the nucleation and growth of CaP in the uniform and narrow channels of the microreactors in the microemulsion system [9]. Moreover, emulsion droplets can also inhibit excess agglomeration of particles, since the surfactants can be absorbed onto the surface of particles [10,11]. However, properties of formulations are influenced by various factors, such as the pH value of solution, ion concentration, stirring rate, reaction time and reaction temperature [12,13]. Up to now, many researchers focusing on the influence of a single factor on particle size have investigated the preparation conditions of CaP/pDNA nanoparticles; nevertheless, statistical methods were rarely employed to optimize preparation conditions.

In order to prepare nano-sized CaP/pDNA particles, the current research adopted the reverse microemulsion to prepare CaP/pDNA nanoparticles (Fig. 1). The formulations were optimized using the three-factor three-level Box–Behnken design. Furthermore, the characters of the optimized CaP/pDNA nanoparticles, *in vitro* release, *in vitro* cell cytotoxic, and transfection were further evaluated.

2. Materials and methods

2.1. Materials

Analytical-grade calcium chloride (99.99%) and sodium phosphate were purchased from Aldrich. *n*-Butyl alcohol, cyclohexane and Triton X-100 were provided by Sinopharm (Shanghai, China). Reporter plasmid pDsRed-M-N1 was a gift from Tsinghua University. Endo-free Plasmid mini kits were purchased from Omega Bio-Tek (USA). Dulbecco's minimum essential medium (DMEM) growth medium, fetal bovine serum (FBS) and penicillin–streptomycin (P/S) were offered by Gibco (USA). Hoechst 33258 was obtained from the Beyotime Institute of Biotechnology (Haimen, Jiangsu, China). Lipofectamine 2000 was purchased from Invitrogen Life Technologies (USA). All other chemicals were commercially available reagents of at least analytical grade.

2.2. Preparation of CaP/pDNA nanoparticles

According to previous reported literatures, Triton X-100 and Butanol were used as mixed emulsifiers; hexane was used as oil phase; 100 μl of calcium chloride solution (1.0M) and 500 ng of pDNA were added to oil phase and stirred for 1 h to prepare microemulsion A. In the same way, 100 μl of Na_3PO_4 (1.0 M) was added to oil phase and agitated for 1 h to form microemulsion B. The microemulsion B was added to the microemulsion A, and the resulting solution was further stirred for another 12 h at a certain speed. Then, the appropriate amount of absolute ethyl alcohol was added to break the emulsion. After that, the mixture was centrifuged for 10 min at 12,000 rpm at 4 °C. The sediment was resuspended in redistilled water after being washed with absolute ethyl alcohol for three times.

2.3. Optimization of CaP/pDNA nanoparticles using Box–Behnken design

Based on single factor study, we choose three main technological factors, the concentration ratio of Ca^{2+} to PO_4^{3-} (X_1), the pH (X_2), and the stirring speed (X_3), to evaluate the interaction effects of those factors in the formulations. The particle size (Y) was chosen as the response. Then, the Box–Behnken design (3-factor, 3-level) was used to optimize the test and a total of 17 experimental runs were generated by Design-Expert software. All variables were investigated at three different levels (Table 1).

Table 1 – Central composite design factors and levels.

Factors	Range and levels		
	−1	0	1
X_1	100	200	300
X_2	7	9	11
X_3	400	600	800

2.4. Characterization of nanoparticles

2.4.1. Particle size analysis

Particle sizes of CaP/pDNA nanoparticles were measured by dynamic light scattering method (Malvern, Worcestershire, UK) with a computerized inspection system at 25 ± 1 °C and at a scattering angle of 90°. All sizes were taken in triplicate and the mean diameter was expressed as intensity diameter.

2.4.2. Transmission electron microscopy

The morphology of CaP/pDNA nanoparticles was observed by transmission electron microscopy (TEM, Tecnai G220, FEI, USA). Freshly prepared calcium phosphate nanoparticles were diluted with water and then dropped in the copper mesh wherein the surface was covered by carbon membrane. Phosphotungstic acid (2.0%) was used for negative dyeing, and the morphology and size of calcium phosphate were observed under the transmission electron microscope.

2.4.3. Entrapment efficiency (E%)

The entrapment efficiency was determined via fluorescence method. The CaP/pDNA nanoparticles in the microemulsion were separated by ultracentrifugation (13,000 rpm for 1 h at 4 °C) and dissolved in acidic buffer (pH 5.5) after washing. The amount of pDNA released from the nanoparticles $[DNA]_r$ was estimated using Hoechst 33258 fluorescence analytical methods. The entrapment efficiency (E%) was calculated by the following equation: $E\% = [DNA]_r/[DNA]_0 \times 100\%$, and all experiments were repeated in triplicate.

2.5. Release of pDNA in vitro

The release of pDNA from the nanoparticles is an important parameter for determining the efficacy of a gene delivery system. Release of pDNA was investigated in this study. In brief, the nanoparticles containing 500 ng of pDNA were suspended in 1 mL release medium at pH 7.4 or 5.5 and incubated for different times at 37 °C on a horizontal shaker at 100 rpm. Samples were taken at each time point, the nanoparticle suspensions were centrifuged at 13,000 rpm, and the supernatant was completely withdrawn. The amount of the pDNA released in the supernatant was determined by Hoechst 33258 staining assay.

2.6. Cell culture

HepG-2 cells were obtained from cell bank of the Chinese Academy of Sciences (Shanghai, China) and maintained in DMEM medium supplemented with 10% FBS and 1% antibiotics (penicillin/streptomycin) at 37 °C in a 5% CO_2 atmosphere.

2.7. In vitro cytotoxicity assays

The cytotoxicity of blank CaP nanoparticles, pDNA and CaP/pDNA against HepG-2 cells was investigated by the standard MTT assay. HepG-2 cells (1×10^4 cells/well) were seeded in 96-well plates and subsequently cultured overnight. Then, cells were treated with CaP, pDNA and CaP/pDNA. After cells were incubated for different times, 20 μl of MTT (5 mg/ml) was added to each well. The cells were further incubated for 4 h and then 150 μl of DMSO was added to dissolve the formazan crystals formed in the live cells. The absorbance of the samples was measured at 490 nm. The results were expressed as percentage viability of control cells and were taken in triplicate.

2.8. In vitro transfection and red fluorescence protein (RFP) quantification

The transfection efficiency of nanoparticles was assessed in HpeG-2 cells. The cells were seeded at a density of 4×10^5 cells/well into 6-well plates. When HpeG-2 cells grew to about 80% confluence, the medium was removed and washed twice with PBS. Then, the CaP/pDNA nanoparticles, free pDNA, Lipofectamine in free FBS DMEM were added to the cells with a final pDNA concentration of 500 ng/well. After a 4-h incubation, the cell culture medium was replaced with fresh serum medium and the cells were allowed to incubate for different times. Then, cells were rinsed twice with PBS and treated with Hoechst 33258 (10 mg/ml) at 37 °C for 30 min, followed by washing with PBS (pH 7.4) and soaking in 4% paraformaldehyde for 30 min. The transfection and expression of red fluorescence protein were determined using a laser scan confocal microscope (LSCM, Olympus, Japan) and quantified by flow cytometry (BD Bioscience, Bedford, MA).

3. Results and discussion

3.1. Nanoparticle preparation and optimization

Based on our previous research, the optimized reverse microemulsion method was used to prepare CaP/pDNA nanoparticles. It was well known that the size of CaP/pDNA was critically related to synthetic methods and synthetic parameters. Especially, parameters like initial concentration, Ca/P molar ratio of the precursors [14], reaction temperature, initial and final pH values, aging time and stirring speed in solution played critical roles in modulating the size and size distribution of CaP/pDNA nanoparticles [15,16].

In order to balance the relationships between those factors and prepare equally distributed nano-sized CaP/pDNA particles, three significant parameters were chosen (X_1: the concentration ratio of Ca^{2+} to PO_4^{3-}, X_2: the system pH, X_3: the stirring speed) to optimize the preparation conditions using the Box–Behnken design methods [17,18]. This design was suitable for exploring quadratic response surfaces and constructing second order polynomial models. Each factor was assigned to three different levels as low, middle and high, respectively, which were listed in Table 1. All possible combinations were shown in Table 2. According to the Box–Behnken design, 17 experimental runs were carried out in random order. Analysis of variance for the response surface and the quadratic model were shown in Table 3.

As shown in the results, the model *F*-value of 16.56 implied that the model was significant. Values of "Prob > *F*" less than 0.050 indicated that model terms were significant. In this study "Prob > *F*" was 0.0006, which suggested that there was only a 0.06% chance that a "model *F*-value" could occur due to noise. The *P*-value for "Lack of Fit" test was 0.1476 which implied that the Lack of Fit was not significantly relative to the pure error,

Table 2 – Central composite design experimental design and results.

Run	Factor 1 X_1	Factor 2 X_2	Factor 3 X_3	Response Y (nm)
1	100	7.00	600.00	67.23
2	200	9.00	600.00	59.23
3	200	9.00	600.00	61.08
4	200	11.00	400.00	73.25
5	100	9.00	400.00	65.57
6	200	7.00	800.00	62.35
7	300	7.00	600.00	68.58
8	200	9.00	600.00	61.76
9	100	11.00	600.00	71.64
10	300	11.00	600.00	75.68
11	200	7.00	400.00	71.09
12	100	9.00	800.00	63.77
13	200	9.00	600.00	62.05
14	300	9.00	800.00	68.24
15	300	9.00	400.00	70.29
16	200	9.00	600.00	60.28
17	200	11.00	800.00	69.23

Note: X_1: representative of the ratio of Ca^{2+} and PO_4^{3-}; X_2: the pH of system; X_3: the stirring speed.

indicating the quadratic model was adequate. As shown in Table 3, X_1, X_2, X_3, X_1^2, X_2^2, X_3^2 were significant model terms. The equation relating to responses of particle size by the design was given below:

$$Y = 229.21375 - 0.16796X_1 - 27.96687X_2 - 0.10058X_3 + 3.36250E - 003X_1X_2 - 3.12500E006X_1X_3 + 2.95000E - 003X_2X_3 + 3.94500E - 004X_1^2 + 1.48937X_2^2 + 5.35625E - 005X_3^2 \quad (R^2 = 0.9551, P = 0.0001).$$

This regression equation described quantitatively the effects of three independent variables (X_1, X_2, X_3) on index and their correlations. It could be predicted to obtain response value of a random formula within the range of designed factor and level by regression equations. This model could be used to navigate the design space.

Table 3 – Analysis of variance table.

Source	Sun of squares	df	Mean square	*F* value	*P*-value Prob > *F*
Model	377.96	9	42.00	16.56	0.0006
X_1	26.57	1	26.57	10.48	0.0143
X_2	52.79	1	52.79	20.81	0.0026
X_3	34.49	1	34.49	13.60	0.0078
X_1X_2	1.81	1	1.81	0.71	0.4263
X_1X_3	0.016	1	0.016	6.160E–003	0.9396
X_2X_3	5.57	1	5.57	2.20	0.1820
X_1^2	65.53	1	65.53	25.83	0.0014
X_2^2	149.44	1	149.44	58.91	0.0001
X_3^2	19.33	1	19.33	7.62	0.0281
Residual	17.76	7	2.54		
Lack of fit	12.49	3	4.16	3.16	0.1476
Pure error	5.27	4	1.32		
Cor Total	395.72	16			

In the experimental process, the three independent variables would interact with other levels. Fig. 2A–C shows that the particle size was investigated when two variables were kept in the experimental range and the other variable was fixed. The three graphs had similar trends, particle size decreased with the increase of each variable, then increased after a critical value. All of them had a lowest point in three-dimensional graph, illustrating that the size of particles had a minimum value in the experimental range. During the preparation of CaP/pDNA nanoparticles, the three factors interacted with each other. As reported, the ratio of Ca to P affected nucleation and crystal growth, while the pH changed crystal nucleus formation conditions and different crystal nucleus morphology. Moreover, the stirring speed could affect the movement rate of ions and nucleation rate of crystals. In conclusion, all those factors could result in the change of particle sizes by a different mechanism. Finally, we intuitively and clearly found out the point of minimum value of the three dimensional graphs.

Based on the studies above, the optimized experimental conditions were shown as follows: the ratio between the calcium to phosphorus (Ca:P) was 179.59, the pH was 8.48, and the stirring speed was 710.75. Optimized nanoparticle formulation had mean size of 60.23 nm, PDI was 0.252, almost the same as the predicted value of 59.79. Therefore, the results of the experiments were close to the predicted values obtained from optimization analysis using desirability function, suggesting that the results of optimization were reliable and reasonable.

3.2. *Characterization of CaP/pDNA nanoparticles*

CaP/pDNA nanoparticles were prepared using the optimal method. Hoechst 33258 fluorescence analytically showed that the encapsulation efficiency (EE %) was around 90%. The size distribution and particle size of the CaP/pDNA nanoparticles were measured with Mastersizer 2000. Fig. 3A shows that the nanoparticles had small particle size and uniform distribution. The mean particle size was 60.23 ± 4.72 nm, and the polydispersity index was 0.252. The size and morphology of nanoparticles were further characterized by TEM. Fig. 3B shows that nanoparticles had spherical-like morphology and uniform particle size.

3.3. *Release of pDNA in vitro*

It was well known that the release of pDNA from nanoparticles served as an important parameter for determining the efficacy of a gene delivery system [19]. Therefore, the release of pDNA from nanoparticles was investigated at different pH in this study. Fig. 4 shows the results of pDNA release from nanoparticles at different pH values. The pDNA release study indicated that very few encapsulated pDNA (less than 10.27%) released from the nanoparticles at pH 7.4. The pDNA release rate increased remarkably when the pH decreased to 5.5. At pH 5.5, more than 50% of the encapsulated pDNA released from nanoparticles at the first 2 h, and more than 90% of the encapsulated pDNA released at 12 h. The pH-dependent manner indicated that nanoparticles could prevent pDNA graduating and increase the pDNA stability in physiological environment. Moreover, the result supported the supposition that

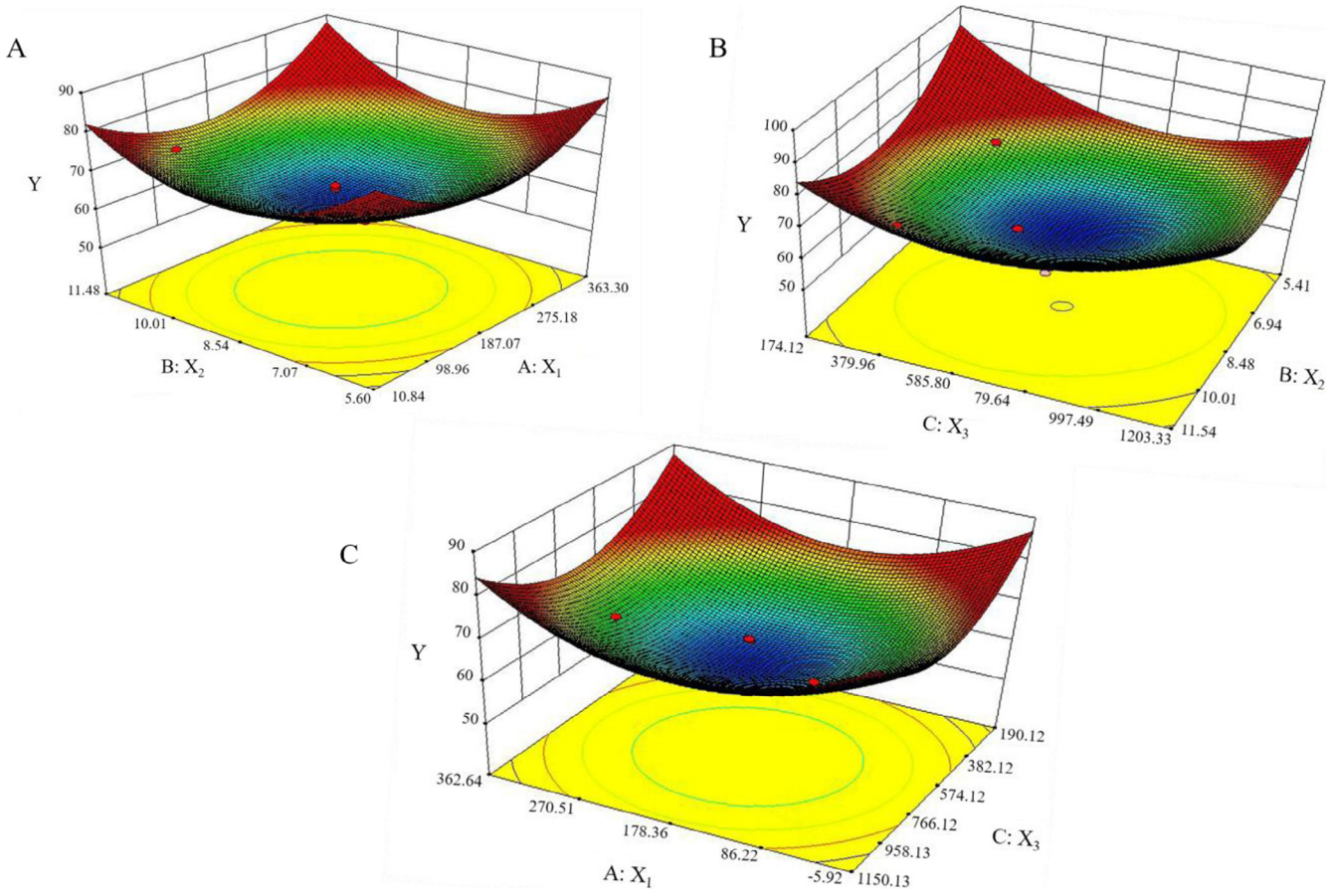

Fig. 2 – 3-D surface response diagrams. (A) Response surface plot for the effect of the ratio of the Ca^{2+} to the PO_4^{3-} and the pH on the particle size. (B) Response surface plot for the effect of the pH and the stirring speed on the particle size. (C) Response surface plot for the effect of the ratio of the Ca^{2+} to the PO_4^{3-} and the stirring speed on the particle size.

nanoparticles could dissociate in the weak acidic environment (pH 5.5).

3.4. *Cytotoxicity of complexes*

In this research, the toxic effects of CaP/pDNA nanoparticles against HepG-2 cells were determined using MTT assay. Fig. 5 shows that the CaP nanoparticles, pDNA and CaP/pDNA nanoparticles did not exhibit any significant cytotoxicity against HepG-2 cells at 24 h ($P > 0.05$); the cell viability was greater than 97%. Although the viability of HepG-2 cells for 48 h and 72 h was slightly lower than that for 24 h, they had no statistical differences ($P > 0.05$) between each time points. Some researchers have reported that intracellular calcium concentration would lead to cell death [20], but there were some other research that reported that increased intracellular Ca^{2+} would pump out of cells by Ca^{2+} pumps, this mechanism would overcome calcium toxicity [21]. These findings further confirmed that CaP/pDNA nanoparticles were safe and biocompatible *in vitro*.

3.5. *In vitro transfection and expression studies*

It was well understood that transfection and expression efficiency of exogenous gene depended on various factors such as complex size and morphology, stability in solutions, ability to bind and release pDNA, cytotoxicity and biocompatibility [22]. In this investigation, *in vitro* transfection and expression of RFP were determined in HepG-2 cells by LSCM and flow cytometry. Fig. 6A shows the expression of RFP after being treated with CaP/pDNA nanoparticles at different times. The results showed that the transfection efficiency of packaged pDNA was time dependent. When cells were treated with nanoparticles for 1 h, there was no RFP produced, the fluorescence intensity was invisible and therefore negligible, but the fluorescence intensity increased after 2 h. Fig. 6B shows that there was a difference in fluorescence intensity among these three groups. No fluorescence was found in free pDNA; in contrast, the fluorescence of optimized CaP/pDNA nanoparticles was stronger than pDNA. But the fluorescence intensity is slightly weaker than Lipofectamine. The pDNA expression was also quantified by flow cytometry. Fig. 6C shows that the results are in accord with the experimental results of LSCM. Therefore, this study identified that optimized CaP/pDNA nanoparticles have the same expression ability with Lipofectamine 2000 because optimized CaP carriers could protect pDNA from being degraded after being entrapped in endosomes by its pH-sensitivity [23].

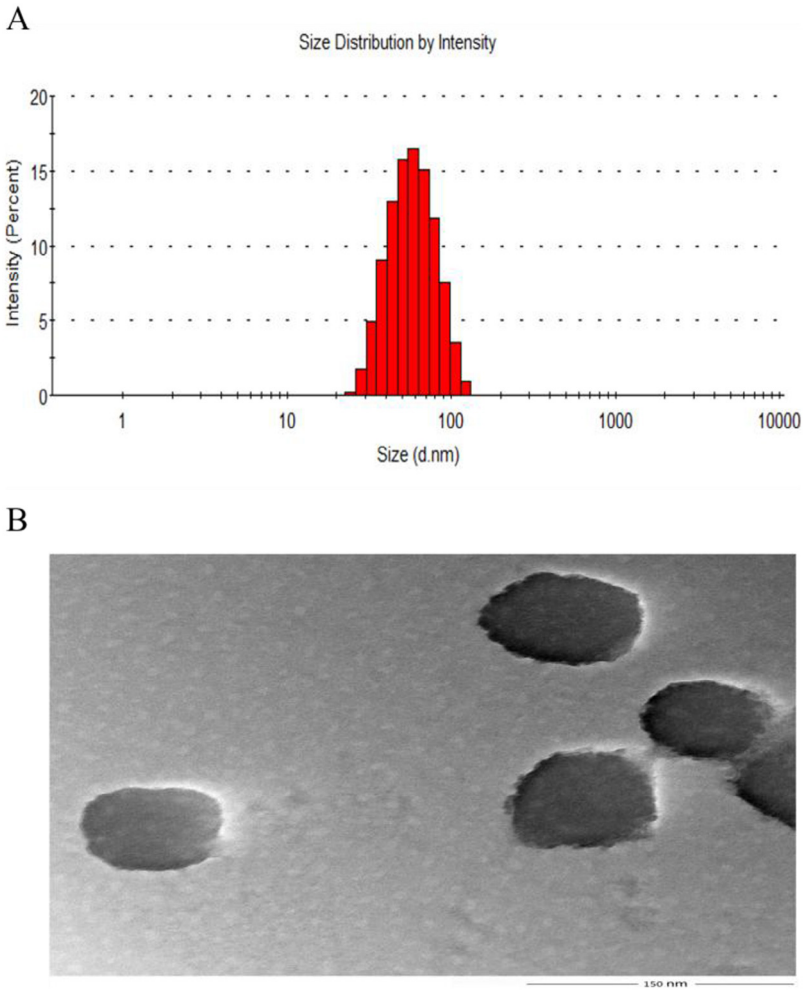

Fig. 3 – Characterization of nanoparticles. (A) The particle size measured by DLS (*n* = 3). (B) Transmission electron micrographs of nanoparticles.

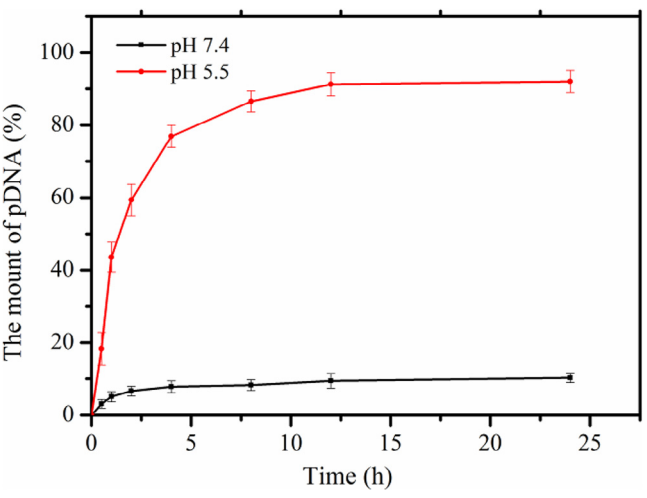

Fig. 4 – The pH-sensitive release of pDNA from nanoparticles at different time points in pH 7.4 and pH 5.5 environment (*n* = 3).

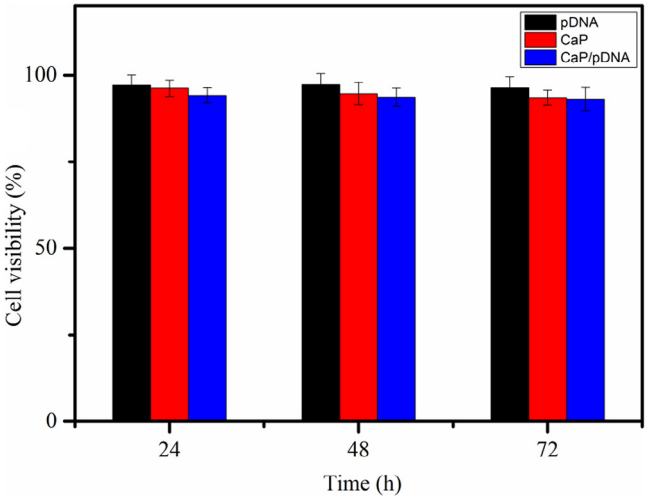

Fig. 5 – *In vitro* cytotoxicity studies of pDNA, CaP and CaP/pDNA nanoparticles (pDNA at 500 ng/well) with different times (*n* = 3).

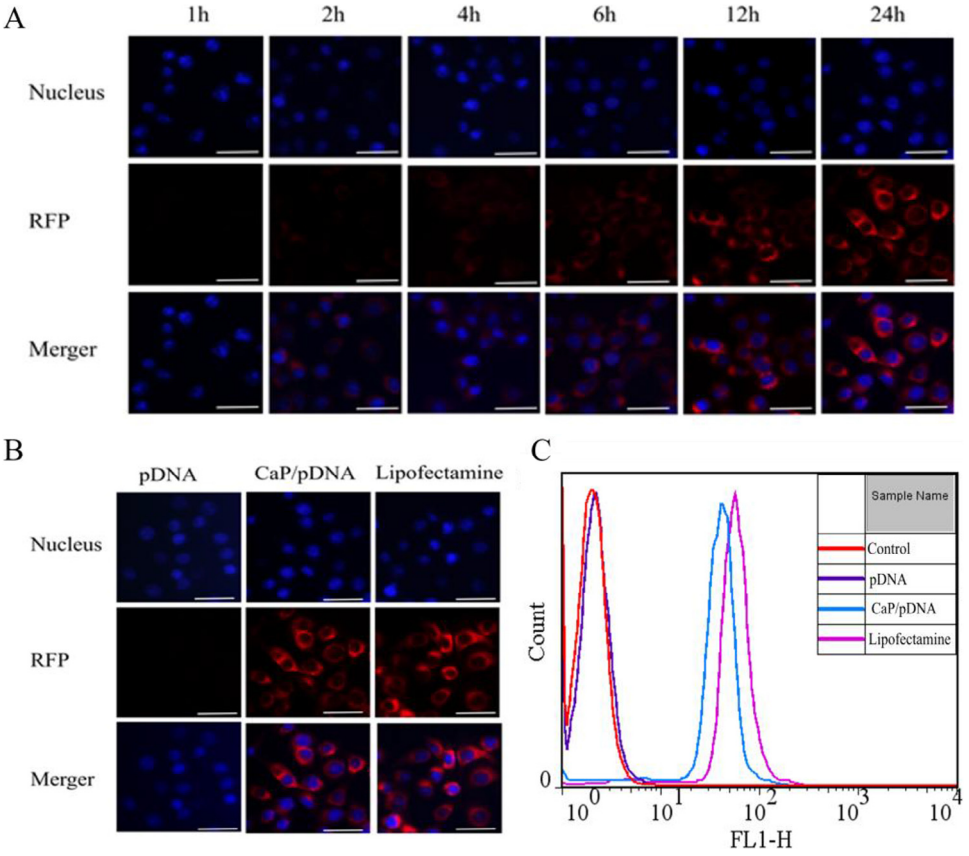

Fig. 6 – (A) *In vitro* transfection and expression of CaP/pDNA nanoparticles at different times (scale bar in all pictures indicates 20 μm). (B) *In vitro* transfection and expression of pDNA, CaP/pDNA, Lipofectamine after 24 h. (C) Imaging flow cytometry results of pDNA, CaP/pDNA, Lipofectamine transfect and express in HepG-2 cells after 24 h ($n = 3$).

4. Conclusion

In the present study, the CaP/pDNA nanoparticles were prepared using reverse microemulsion method and optimized with employing Box–Behnken design. The nanoparticle size was close to the predicted one generated by Design. The optimized nanoparticles had smaller particle size, uniform distribution and higher encapsulation efficiency. The MTT results showed that the optimized CaP/pDNA nanoparticles had better biocompatibility *in vitro*. *In vitro* transfection study indicated that optimized formulations showed good transfection efficiency. We could draw a conclusion that Box–Behnken design method could be used in the optimization of nano-sized CaP/pDNA particles.

Acknowledgments

The authors alone are responsible for the content and writing of this article. The authors are grateful to the Natural Science Foundation Committee of China for the financial support (No. 81173004 and No. 81202483).

REFERENCES

[1] Jordan M, Wurm F. Transfection of adherent and suspended cells by calcium phosphate. Methods 2004;33:136–143.
[2] Uskoković V, Uskoković DP. Nanosized hydroxyapatite and other calcium phosphates: chemistry of formation and application as drug and gene delivery agents. J Biomed Mater Res B Appl Biomater 2011;96:152–191.
[3] Chen Q, Wong C, Lu W, et al. Strengthening mechanisms of bone bonding to crystalline hydroxyapatite in vivo. Biomaterials 2004;25:4243–4254.
[4] Oyane A, Wang X, Sogo Y, et al. Calcium phosphate composite layers for surface-mediated gene transfer. Acta Biomater 2012;8:2034–2046.
[5] Pedraza CE, Bassett DC, McKee MD, et al. The importance of particle size and DNA condensation salt for calcium phosphate nanoparticle transfection. Biomaterials 2008;29:3384–3392.
[6] Sadat-Shojai M, Khorasani M-T, Dinpanah-Khoshdargi E, et al. Synthesis methods for nanosized hydroxyapatite with diverse structures. Acta Biomater 2013;9:7591–7621.
[7] Lin K, Wu C, Chang J. Advances in synthesis of calcium phosphate crystals with controlled size and shape. Acta Biomater 2014;10:4071–4102.

[8] Chowdhury EH, Kunou M, Nagaoka M, et al. High-efficiency gene delivery for expression in mammalian cells by nanoprecipitates of Ca–Mg phosphate. Gene 2004;341:77–82.
[9] Perez-Coronado A, Calvo L, Alonso-Morales N, et al. Multiple approaches to control and assess the size of Pd nanoparticles synthesized via water-in-oil microemulsion. Colloids Surf A Physicochem Eng Asp 2016;497:28–34.
[10] Kandori K, Kuroda T, Togashi S, et al. Preparation of calcium hydroxyapatite nanoparticles using microreactor and their characteristics of protein adsorption. J Phys Chem B 2010;115:653–659.
[11] Zhou W, Wang M, Cheung W, et al. Synthesis of carbonated hydroxyapatite nanospheres through nanoemulsion. J Mater Sci Mater Med 2008;19:103–110.
[12] Guo G, Sun Y, Wang Z, et al. Preparation of hydroxyapatite nanoparticles by reverse microemulsion. Ceram Int 2005;31:869–872.
[13] Koumoulidis GC, Katsoulidis AP, Ladavos AK, et al. Preparation of hydroxyapatite via microemulsion route. J Colloid Interface Sci 2003;259:254–260.
[14] Olton D, Li J, Wilson ME, et al. Nanostructured calcium phosphates (NanoCaPs) for non-viral gene delivery: influence of the synthesis parameters on transfection efficiency. Biomaterials 2007;28:1267–1279.
[15] Bouladjine A, Al-Kattan A, Dufour P, et al. New advances in nanocrystalline apatite colloids intended for cellular drug delivery. Langmuir 2009;25:12256–12265.
[16] Jokić B, Mitrić M, Radmilović V, et al. Synthesis and characterization of monetite and hydroxyapatite whiskers obtained by a hydrothermal method. Ceram Int 2011;37:167–173.
[17] Mokhtar WNAW, Bakar WAWA, Ali R, et al. Optimization of extractive desulfurization of Malaysian diesel fuel using response surface methodology/Box–Behnken design. J Ind Eng Chem 2015;30:274–280.
[18] Dizaj SM, Lotfipour F, Barzegar-Jalali M, et al. Box-Behnken experimental design for preparation and optimization of ciprofloxacin hydrochloride-loaded $CaCO_3$ nanoparticles. J Drug Deliv Sci Technol 2015;29:125–131.
[19] Jang S, Lee S, Kim H, et al. Preparation of pH-sensitive CaP nanoparticles coated with a phosphate-based block copolymer for efficient gene delivery. Polymer (Guildf) 2012;53:4678–4685.
[20] Mattson MP, Chan SL. Calcium orchestrates apoptosis. Nat Cell Biol 2003;5:1041–1043.
[21] Tseng Y-C, Yang A, Huang L. How does the cell overcome LCP nanoparticle-induced calcium toxicity? Mol Pharm 2013;10:4391–4395.
[22] Lee D, Ahn G, Kumta PN. Nano-sized calcium phosphate (CaP) carriers for non-viral gene/drug delivery. Nano Drug Deliv Imaging Tissue Eng 2013;203–236.
[23] Lee D, Upadhye K, Kumta PN. Nano-sized calcium phosphate (CaP) carriers for non-viral gene delivery. Mater Sci Eng B 2012;177:289–302.